Journal of Electronic Materials

Optimization of Al2O3 and Li3BO3 content as sintering additives of Li7La2.95Ca0.05ZrTaO12 at low temperature

--Manuscript Draft--

Manuscript Number:	JEMS-D-16-00822R1
Full Title:	Optimization of Al2O3 and Li3BO3 content as sintering additives of Li7La2.95Ca0.05ZrTaO12 at low temperature
Article Type:	Original Research
Keywords:	Ca-Ta doped LLZ; sintering additives; Al2O3; Li3BO3; Li ion conductivity
Corresponding Author:	Nataly Carolina Rosero Navarro, Dr. Hokkaido University Sapporo, Hokkaido JAPAN
Corresponding Author Secondary Information:	
Corresponding Author's Institution:	Hokkaido University
Corresponding Author's Secondary Institution:	
First Author:	Nataly Carolina Rosero Navarro, Dr.
First Author Secondary Information:	
Order of Authors:	Nataly Carolina Rosero Navarro, Dr. Akira Miura, Dr. Mikio Higuchi, Dr. Kiyoharu Tadanaga, Dr.
Order of Authors Secondary Information:	
Funding Information:	Japan Society for the Promotion of Science (P13371) — Dr. Nataly Carolina Rosero Navarro
Abstract:	Simultaneous effect of Al2O3 and Li3BO3 addition on sintering behavior and Li-ion conductivity of Li7-xLa2.95Ca0.05ZrTaO12 (LLCZT) garnet electrolyte sintered at 900 °C (10 h) is evaluated. Crystal phase and microstructure of the different composites were evaluated by X-ray diffraction (XRD) and scanning electron microscopy (SEM), respectively. Electrical properties of the composites with high relative densities (95 %) were examined by impedance spectroscopy (EIS). Cubic phase was formed for LLCZT sintered with 0 - 0.21 moles of Al2O3 and 0.70 - 0.80 moles of Li3BO3. The excess of Al2O3 (0.22 moles) led to the formation of secondary phases. SEM observation revealed the good interconnection between LLCZT grains and the distribution of the glassy phase formed by Li3BO3 and Al2O3. Effective combination of 0.21 moles of Al2O3 and 0.80 moles of Li3BO3 produced denser material with high relative density of 95 % and high Li-ion conduction of 1 × 10-4 S/cm at 32 °C.

Optimization of Al_2O_3 and Li_3BO_3 content as sintering additives of $Li_{7-x}La_{2.95}Ca_{0.05}ZrTaO_{12}$ at low temperature

Nataly Carolina Rosero-Navarro*, Akira Miura, Mikio Higuchi and Kiyoharu Tadanaga

Division of Applied Chemistry, Faculty of Engineering, Hokkaido University, Sapporo, Japan

(*) Corresponding author:

Kita 13 Nishi 8, Kita-ku, Sapporo 060-8628, Japan

Division of Applied Chemistry

Faculty of Engineering, Hokkaido University

e-mail: rosero@eng.hokudai.ac.jp, karolrosero@gmail.com (N.C. Rosero-Navarro)

tel. +81 11-706-6574

Abstract

Simultaneous effect of Al_2O_3 and Li_3BO_3 addition on sintering behavior and Li-ion conductivity of $Li_{7-x}La_{2.95}Ca_{0.05}ZrTaO_{12}$ (LLCZT) garnet electrolyte sintered at 900 °C (10 h) is evaluated. Crystal phase and microstructure of the different composites were evaluated by X-ray diffraction (XRD) and scanning electron microscopy (SEM), respectively. Electrical properties of the composites with high relative densities (95 %) were examined by impedance spectroscopy (EIS). Cubic phase was formed for LLCZT

sintered with 0 – 0.21 moles of Al_2O_3 and 0.70 – 0.80 moles of Li_3BO_3. The excess of Al_2O_3 (0.22 moles) led to the formation of secondary phases. SEM observation revealed the good interconnection between LLCZT grains and the distribution of the glassy phase formed by Li_3BO_3 and Al_2O_3. Effective combination of 0.21 moles of Al_2O_3 and 0.80 moles of Li_3BO_3 produced denser material with high relative density of 95 % and high Li-ion conduction of 1×10^{-4} S/cm at 32 °C.

Introduction

Garnet-type solid electrolytes have been studied extensively [1,2], because high ionic conductivity at room temperatures (10^{-3} - 10^{-4} S/cm), high chemical stability against Li metal and wide potential windows with electrochemical decomposition voltage of ~6 V vs. elemental Li anode. Typical temperatures around 1200 °C are used to sinter the material and stabilize the cubic phase responsible of the high conductivity. At these temperatures, the control of the concentration of the lithium into garnet structure is the major challenge. Control of the stoichiometry composition through reduction of sintering temperature as well as processing periods has been led by chemical substitution and the use of sintering additives. $Li_7La_3Zr_2O_{12}$ (LLZ) garnet prepared by the conventional solid state reaction (SSR) at 1230 °C (36 h) exhibits a total Li-ion conductivity of 2.4×10^{-4} S/cm at 25 °C with a bulk conductivity of 4.7×10^{-4} S/cm [3]. Partial substitution of Zr by elements such as Nb, Ta and Te produces an improvement of Li-ion conductivity in more than 3 times. Li-ion conductivities of $Li_{6.75}La_3Zr_{1.75}Nb_{0.25}O_{12}$ [4] (1200 °C, 36 h), $Li_{6.4}La_3Zr_{1.4}Ta_{0.6}O_{12}$ [5] (1140 °C, 16 h) and $Li_{6.4}La_3Zr_{1.75}Te_{0.25}O_{12}$ [6] (1100 °C, 15 h) have reached 8×10^{-4} S/cm, 10×10^{-4} S/cm and 10.2×10^{-4} S/cm, respectively. Further,

simultaneous doping with other elements such as Ba has led to materials with high Li-ion conductivity at lower sintering temperatures, where $Li_{6.5}La_{2.5}Ba_{0.5}ZrTaO_{12}$ [7] (1100 °C, 6 h) achieves Li-ion conductivities of 2×10^{-4} S/cm (bulk). Although the Li content in the unit formula (6.4 – 6.75) is slightly lower than that of LLZ [3], conductivity remains high in the order of 10^{-3}–10^{-4} S/cm. The enhanced Li-ion conductivity has been attributed to optimized lithium content in octahedral and tetrahedral sites of the garnet structure [1].

Regarding to sintering additives, elements such as aluminum have proved to be effective to improve the densification of the material at lower sintering temperatures. Geiger et al. [8] are one of the first groups to note the contamination by Al from the crucible during sintering process and its influence on the stabilizing of the cubic garnet phase. Alternatively, other researches have revealed that the Al acts as a sintering additive by residing in the grain boundaries and also inside of the grain creating more Li-ion vacancies improving the Li-ion conductivity [9-11]. Li-ion conductivity of $Li_{6.625}La_3Zr_{1.625}Ta_{0.375}O_{12}$ sintered at 1000 °C (24 h) with 29 mol% Al [12] reaches 5×10^{-4} S/cm. Other compounds used as sintering additives include Li_2O, Li_3BO_3, Li_3PO_4 and Li_4SiO_4 [13-18]. These materials act as binder between the garnet particles during the sintering treatment by the formation of liquid phases at low temperatures, reducing the grain boundary resistance and improving the Li-ion conductivity pathway. Combination of Al and Li_3BO_3 has been reported to be particularly useful to produce denser material at lower sintering temperatures [14,15]. Li-ion conductivity of LLZ sintered at 900 °C (36 h) with 0.3 moles of Al and 0.68 moles of Li_3BO_3 [14] achieves 1×10^{-4} S/cm. High Li-ion conductivity at lower sintering temperatures has been attained using sintering additives in materials with aliovalent substitution of LLZ garnet structure.

Li-ion conductivity of $Li_{6.8}La_{2.95}Ca_{0.05}Zr_{1.75}Nb_{0.25}O_{12}$ sintered at 800 °C (40 h) with 0.2 mol% Al_2O_3 and ≥5 vol.% Li_3BO_3 [15] reaches 3.6×10^{-4} S/cm.

$Li_{7-x}La_{2.95}Ca_{0.05}ZrTaO_{12}$ (LLCZT) garnet electrolyte sintered at 900 °C (10 h) using simultaneous addition of Al_2O_3 and Li_3BO_3 is reported in this work. Although family of Ta doped LLZ garnet materials presents high Li-ion conductivities [2,1], few works have explored the sintering at low temperatures. Low sintering temperature allows the better control of stoichiometry of garnet structure, especially the lithium content and thus, optimized Li-ion conductivity. In this work, sintering behavior was evaluated at 900 ºC with a short dwell time of 10 h. Even though this is not the lowest sintering temperature used to prepare garnet materials [1,2], the treatment was performed at shorter dwell time reported so far.

2. Materials and Methods

2.1 Synthesis of $Li_{7-x}La_{2.95}Ca_{0.05}ZrTaO_{12}$ (LLCZT)

$LiNO_3$ (99%, Kanto Chemical Co.), $La(NO_3)_3 \cdot 6H_2O$ (99.99%, Kanto Chemical Co.), $Zr(OC_4H_9)_4$ (85% in butanol, Wako) and $Ta(OC_2H_5)_5$ (99.999%, High Purity Chemicals) without further purification were used as precursors. The ethylacetoacetate (EAC, 99.0%, Kanto Chemical Co.) was used as a stabilizing agent for the alkoxides. Molar ratio between Li:La:Zr:Ta:EAC was 7:3:1:1:1.6. Ethanol (99.5%, Wako) was used as solvent. The lithium and lanthanum salts were dissolved in ethanol ($LiNO_3$ 3.85 M). Separately, the zirconium and tantalum alkoxides were mixed and reacted with stabilizing agent. Then both solutions were mixed. The final solution was stirred at 25 °C. Solvent in the solution was evaporated at 80 °C for 24 h to obtain a gel. Dry gel was ground and calcined at 700 °C for 5 h at heating rate of 1 °C/min. The calcined

powders were attrition-milled in a ZrO_2 pot with 2 mm diameter ZrO_2 balls in a toluene medium at 300 RPM for 6 h using a planetary ball mill.

2.2 Preparation of pellets

Li_3BO_3 [18] and Al_2O_3 (1 μm, 99.99% High Purity Chemicals) were added to the calcined powder of LLCZT by hand-milling in an agate mortar. The evaluated additive concentrations of Li_3BO_3 were 0.70, 0.75, and 0.80 moles (molar ratio of Li_3BO_3 to LLCZT). In the case of Al effect, the evaluated concentrations were 0.11, 0.19, 0.21 and 0.22 moles of Al_2O_3 (molar ratio of Al_2O_3 to LLCZT). The composite powders were pressed at 100 MPa into pellets and were sintered at 700 °C (5 h) and 900 °C (10 h) using a heating rate of 1 °C/min. The composites were sintered under ambient atmosphere using alumina crucibles. The pellets were thoroughly buried in identical powder to mitigate losses of lithium and prevent any additional contamination.

2.3 Characterization

Crystal phase was determined by X-ray diffraction (XRD) using a RINT 2000 Ultima RIGAKU diffractometer. Each sample was scanned between 10° and 60° at a rate of 2°/min using Cu-Kα radiation. Cross section of the pellet, polished using the ion beam cross section polisher, was characterized using scanning electron microscopy (SEM, JMS-6390; JEOL). Relative density was determined by dividing the geometric density by the theoretical density of the composite. Geometric density was determined by the pellet weight and physical dimensions. Theoretical density was calculated using the rule of mixtures, applying the theoretical density of Li_3BO_3 (2.16 g/cm^3) and LLZ (5.1 g/cm^3).

The electrochemical behavior of the pellets was determined using electrochemical impedance spectroscopy (SI1260; Solartron). Impedance spectra were recorded

between 1 and 1 × 10^6 Hz. The measurements were conducted at various temperatures (30–180 °C) in an argon atmosphere. The surface of the as-sintered pellets was polished with sandpaper (#1000). Then, circular golden electrodes (approx. 0.6 cm^2) were sputter-coated onto both sides of the sample. Current collection was done using golden wires.

3. Results and discussion

Figure 1 displays the XRD patterns of LLCZT sintered at 900 °C with 0.80 moles of Li_3BO_3 and different concentration of Al_2O_3. The XRD patterns of the material sintered without any additive and the powder calcined at 700 °C were also included as comparison and reference. Peaks assigned to cubic phase and secondary phase corresponding to $La_2Zr_2O_7$ (pyrochlore) are detected at 700 °C. The pyrochlore phase has been identified as intermediate product during the formation of garnet oxide materials by sol-gel process [18,19]. The formation of pure cubic garnet phase is achieved at 900 °C, in a good agreement with similar material composition sintered at high temperatures (1140 °C) [5]. The addition of Li_3BO_3 and lower concentration of Al_2O_3 (<0.22 moles) does not produce any significant changes in the XRD patterns. A slight shift of XRD peaks to higher diffraction angle respect to LLCZT sintered without additives was observed. Regarding the effect of Li_3BO_3 concentration on the structure of LLCZT, XRD patterns of LLCZT sintered with 0.21 moles of Al_2O_3 and different concentration of Li_3BO_3 (not shown) revealed the formation of pure cubic phase without presence of secondary phases. The absence of secondary phase confirms that both sintering additives, Li_3BO_3 and Al_2O_3, should form a glassy phase in the grain boundary [14,10]. Peaks shifting can be related with the modification of garnet structure by the incorporation of Al during sintering process. Excess of Al_2O_3, ≥0.22 moles, leads to the

formation of secondary phase, $La_2Li_{0.5}Al_{0.5}O_4$, and peaks shifting at lower diffraction angle respect to LLCZT sintered without additives. The Al content used in this work is rather higher than those reported in the literature [20,2,1] used to stabilize the cubic phase of LLZ. Rangasamy et al. [20] determined that 0.204 moles of Al are required to stabilize the cubic phase at 1000 ºC by the conventional solid state reaction, the formation of secondary phases was identified from the addition of 0.389 moles of Al. In the current work, the cubic phase was obtained at lower temperatures without the addition of Al, formation of secondary phases was observed at higher content of Al, 0.44 moles of Al, and pure cubic phase was observed up to 0.42 moles of Al. On the other hand, Rangasamy et al. [20] assigned the secondary phase with $LaAlO_3$ phase, while Düvel et al. [11] observed the formation of $La_2Li_{0.5}Al_{0.5}O_4$ phase in high Al-doped LLZ garnet electrolyte. Despite $La_2Li_{0.5}Al_{0.5}O_4$ phase has been clearly identified (Figure 1), other phases such as $LaAlO_3$ or $LiAlO_2$ could be formed [9].

Table I shows the relative density of LLCZT pellets sintered at 900 °C with Li_3BO_3 and Al_2O_3. The material sintered without additive exhibits a relative density of 56%. The use of Li_3BO_3 achieves only 58% of relative density, negligible in comparison with the material without sintering additives. Higher relative densities are attained with the increase of Al_2O_3 concentration, and the relative density is reached to 95% (0.21 moles), which is circa 30% higher than that of the material without additive or sintering with Li_3BO_3. The use of 0.22 moles of Al_2O_3 produces the drop of relative density to 83%. The decrease of relative density is attributed to the formation of secondary phases, as confirmed by XRD. On the other hand, the reduction of Li_3BO_3 content leads to the decrease, circa of 10%, of relative density. Higher content of Li_3BO_3 could create an unfavorable effect producing the drop of the Li-ion conductivity since the Li-ion

conductivity of Li_3BO_3 is two orders of magnitude lower than that of the LLZ garnet [15,18].

The highest relative density of 95 % was obtained with 0.21 moles of Al_2O_3 and 0.80 moles of Li_3BO_3. Figure 2 shows the SEM and corresponding backscattered electron image of polished cross-section of the LLCZT pellet sintered with 0.21 moles of Al_2O_3 and 0.80 moles of Li_3BO_3. Good interconnection between LLCZT grains is confirmed by bright regions on backscattered electron image. The distribution of the glassy phase formed by Li_3BO_3 and Al_2O_3 is evidenced by dark region on backscattered electron image. Similar results were obtained in Al-doped LLZ and $Li_7La_3ZrNbO_{12}$ garnet oxides sintered with Li_3BO_3 [18,14].

Impedance spectra at 32 ºC for LLCZT sintered at 900 °C with 0.21 moles of Al_2O_3 and 0.80 moles of Li_3BO_3 is shown in Figure 3. The spectra consist of a well-defined semicircle at high frequency and capacitive tale at low frequency (polarization of golden electrodes). This type of impedance spectra is often interpreted as the result of a series association of the bulk resistance of the grains at high frequency and resistance of grain boundary at intermediate frequency. The grain resistance involves components such as LLCZT bulk and Li_3BO_3 bulk, while grain boundary involves LLCZT/LLCZT grain boundary and LLCZT/Li_3BO_3 interface. Thus, it is difficult to separate each resistance components and perform an in-depth analysis of the spectra. The total resistance was determined from the real component of impedance, Z, in the intersection point between the semicircle and the tail produced by the electrodes (4×10^4 Hz). The total (bulk and grain boundary) Li-ion conductivity at 32 ºC is estimated to be 1.04×10^{-4} S/cm. Total Li-ion conductivity is three order of magnitude higher than the material sintered without additives (1×10^{-7} S/cm) and it is comparable to that of Al-doped LLZ pellet sintered

with Li_3BO_3 at 900°C and longer dwell time of 36 h (1×10^{-4} S/cm) [14]. Arrhenius plot (Figure 4) displays total Li-ion conductivity obtained for LLCZT with highest relative density, 0.19 and 0.21 moles of Al_2O_3 and 0.80 moles of Li_3BO_3. The activation energies were estimated to be 0.35 and 0.34 eV for the garnet material sintered with 0.19 and 0.21 moles of Al_2O_3, respectively. These values are in good agreement with other members reported in the garnet-type electrolytes sintered at higher temperatures such as $Li_{6.4}La_3Zr_{1.6}Ta_{0.6}O_{12}$ (1140 °C, 0.35 eV) [5] and $Li_{6.5}La_{2.5}Ba_{0.5}ZrTaO_{12}$ (1100°C, 0.34 eV) [7].

Li-ion conductivity of LLCZT sintered with 0.19 and 0.21 moles was clearly different, despite its similar relative density around 95%. LLCZT sintered with 0.19 moles of Al_2O_3 is one order of magnitude lower respect to the material sintered with 0.21 moles of Al_2O_3. The difference of Li-ion conductivity can be related with the effect of Al on the chemical composition of garnet material. The grain boundary should consist mainly of an amorphous phase of Li-B-Al-O, according to the results of XRD (Figure 1), but diffusion between elements of garnet and glassy phase cannot be ruled out. Liquid phase formed by Li_3BO_3-Al_2O_3 at low temperatures of 700 °C penetrates the solid–solid interfaces and promotes good rearrangement of the particles leading to denser ceramics. During that process, grain growth is helped by grain coalescence and grain-reprecipitation from the small grains to the adjacent large grains. Simultaneous interdiffusion of elements between garnet material and additives is expected during these processes. In fact, Ohta et al. [15] have attributed the high Li-ion conductivity of Al-doped $Li_{6.8}La_{2.95}Ca_{0.05}Zr_{1.75}Nb_{0.25}O_{12}$ electrolyte sintered with Li_3BO_3 to the simultaneous interdiffusion of elements resulted in a grain boundary formed by Li–Ca–B–O phase and grain enriched with Al. It is well known that adequate quantities of Al

can create more Li-ion vacancies [9]. On the other hand, high Al content can affect not only Li sites but garnet network since Al replaces La and Zr sites producing change of Li ion dynamics [11]. Thus, the effect of Al in the garnet structure can produce materials with better Li-ion conductivity.

Densification behavior and Li-ion conductivity are controlled by the optimized interdifussion of elements between liquid phase and garnet material. Effective combination of 0.21 moles of Al_2O_3 and 0.80 moles of Li_3BO_3 contributed to the good distribution of the grains providing good Li-ion conduction pathway of $Li_{7-x}La_{2.95}Ca_{0.05}ZrTaO_{12}$ garnet electrolyte. The garnet electrolyte reported in this work represents one of the materials sintered at low temperature with high conductivity into the family of Ta-doped LLZ garnet-type electrolyte [2].

4. Conclusions

$Li_{7-x}La_{2.95}Ca_{0.05}ZrTaO_{12}$ (LLCZT) garnet electrolyte was sintered at 900 °C (10 h) using Al_2O_3 and Li_3BO_3 as sintering additives. XRD showed the formation of single cubic phase for LLCZT pellets sintered with 0 – 0.21 moles of Al_2O_3 and 0.70 – 0.80 moles of Li_3BO_3. Addition of 0.22 moles of Al_2O_3 led to the formation of $La_2Li_{0.5}Al_{0.5}O_4$ secondary phase. XRD and SEM observation confirmed that material is composed of LLCZT interconnected grains and amorphous phase of Al_2O_3 and Li_3BO_3 in the grain boundary. Combination of 0.21 moles of Al_2O_3 and 0.80 moles of Li_3BO_3 led to denser materials achieving 95 % of relative density and high Li-ion conductivity of 1×10^{-4} S/cm.

Acknowledgements

N.C. Rosero Navarro would like to acknowledge the Japan Society for the Promotion of Science (JSPS) for support and Postdoctoral Fellowship under grant number P13371.

This study was funded by Japan Society for the Promotion of Science. The authors declare that they have no conflict of interest.

Reference

1. J.C. Bachman, S. Muy, A. Grimaud, H.H. Chang, N. Pour, S.F. Lux, O. Paschos, F. Maglia, S. Lupart, P. Lamp, L. Giordano, Y. Shao-Horn, Chem. Rev. 116, 140-162 (2016)

2. V. Thangadurai, S. Narayanan, D. Pinzaru, Chem. Soc. Rev. 43, 4714-4727 (2014)

3. R. Murugan, V. Thangadurai, W. Weppner, Angew. Chem., Int. Ed. 46, 7778-7781 (2007)

4. S. Ohta, T. Kobayashi, T. Asaoka, J. Power Sources 196, 3342-3345 (2011)

5. Y. Li, J.T. Han, C.A. Wang, H. Xie, J.B. Goodenough, J. Mater. Chem. 22, 15357-15361 (2012)

6. C. Deviannapoorani, L. Dhivya, S. Ramakumar, R. Murugan, J. Power Sources 240, 18-25 (2013)

7. S. Narayanan, V. Epp, M. Wilkening, V. Thangadurai, RSC Adv. 2, 2553-2561 (2012)

8. C.A. Geiger, E. Alekseev, B. Lazic, M. Fisch, T. Armbruster, R. Langner, M. Fechtelkord, N. Kim, T. Pettke, W. Weppner, Inorg. Chem. 50, 1089-1097 (2011)

9. Y. Jin, P.J. McGinn, J. Power Sources 196, 8683-8687 (2011)

10. S. Kumazaki, Y. Iriyama, K.H. Kim, R. Murugan, K. Tanabe, K. Yamamoto, T. Hirayama, Z. Ogumi, Electrochem. Commun. 13, 509-512 (2011)

11. A. Düvel, A. Kuhn, L. Robben, M. Wilkening, P. Heitjans, J. Phys. Chem. C. 116, 15192-15202 (2012)

12. H. Buschmann, S. Berendts, B. Mogwitz, J. Janek, J. Power Sources 206, 236-244 (2012)

13. Y. Li, Y. Cao, X. Guo, Solid State Ionics 253, 76-80 (2013)

14. K. Tadanaga, R. Takano, T. Ichinose, S. Mori, A. Hayashi, M. Tatsumisago, Electrochem. Commun. 33, 51-54 (2013)

15. S. Ohta, J. Seki, Y. Yagi, Y. Kihira, T. Tani, T. Asaoka, J. Power Sources 265, 40-44 (2014)

16. N. Janani, C. Deviannapoorani, L. Dhivya, R. Murugan, RSC Adv. 4, 51228-51238 (2014)

17. N. Janani, S. Ramakumar, S. Kannan, R. Murugan, J. Am. Ceram. Soc. 98, 2039-2046 (2015)

18. N.C. Rosero-Navarro, T. Yamashita, A. Miura, M. Higuchi, K. Tadanaga, Solid State Ionics 285, 6-12 (2016)

19. J. Sakamoto, E. Rangasamy, H. Kim, Y. Kim, J. Wolfenstine, Nanotechnology 24, 424005 (2013)

20. E. Rangasamy, J. Wolfenstine, J. Sakamoto, Solid State Ionics 206, 28-32 (2012)

Figure captions

Fig. 1 XRD patterns of LLCZT sintered at 900 °C with 0.80 moles of Li_3BO_3 and different concentration of Al_2O_3. Circles denotes LLCZT cubic phase, square and asterisk denote secondary phases of $La_2Zr_2O_7$ and $La_2Li_{0.5}Al_{0.5}O_4$, respectively.

Fig. 2 SEM and backscattered electron image of polished cross-section of LLCZT sintered at 900 °C with 0.80 moles of Li_3BO_3 and 0.21 moles of Al_2O_3.

Fig. 3 Nyquist plot at 32 ºC of pellet prepared with LLCZT sintered with 0.80 moles of Li_3BO_3 and 0.21 moles of Al_2O_3.

Fig. 4 Arrhenius plots for the total (bulk + grain-boundary) electrical conductivity of LLCZT sintered with 0.80 moles of Li_3BO_3 and different concentrations of Al_2O_3.

Table caption

Table I. Relative density of LLCZT sintered at 900 °C with Li_3BO_3 and Al_2O_3.

Figure 1

Click here to download Figure Figure 1.jpg

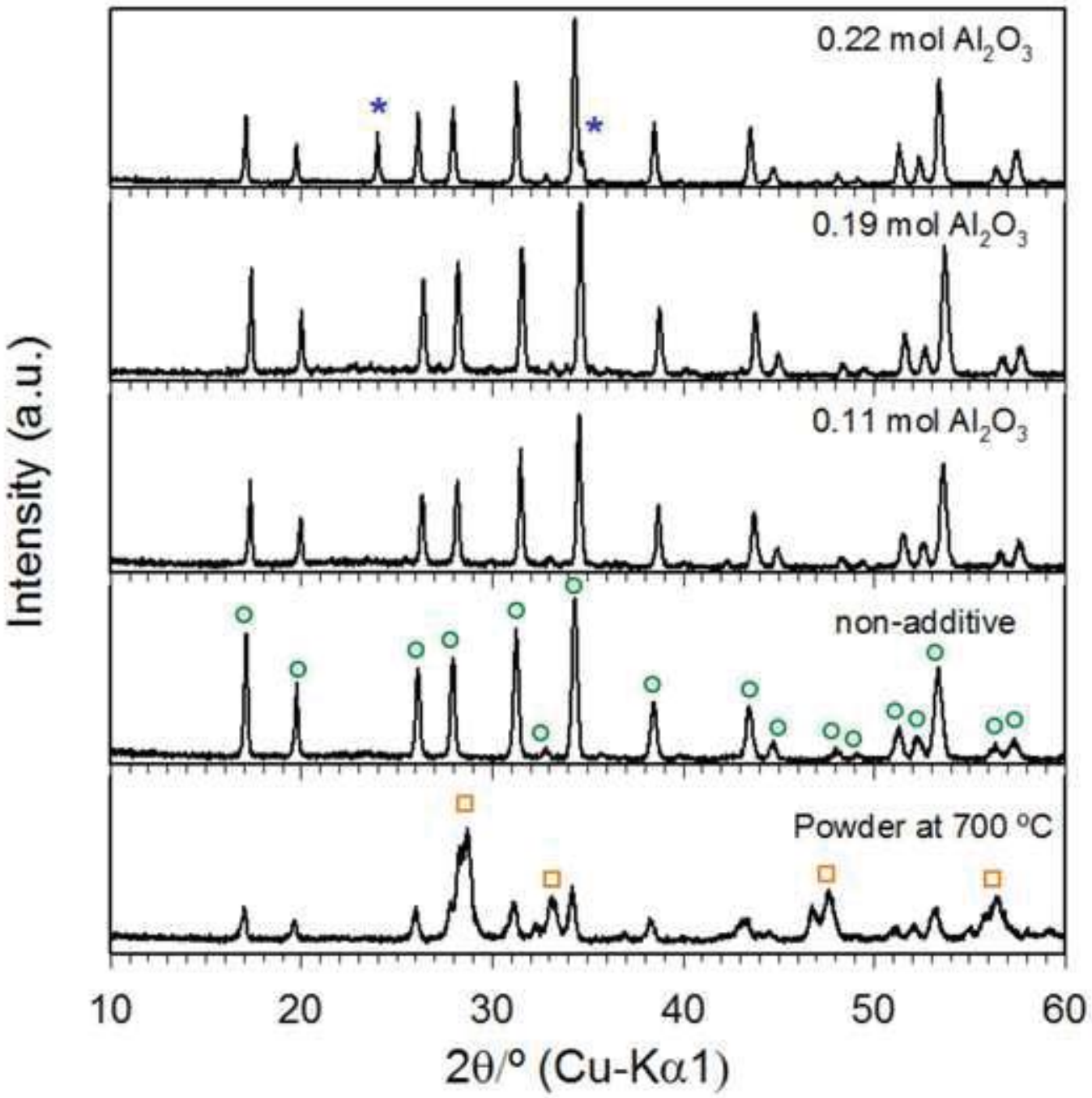

Figure 2

Click here to download Figure Figure 2_change.jpg

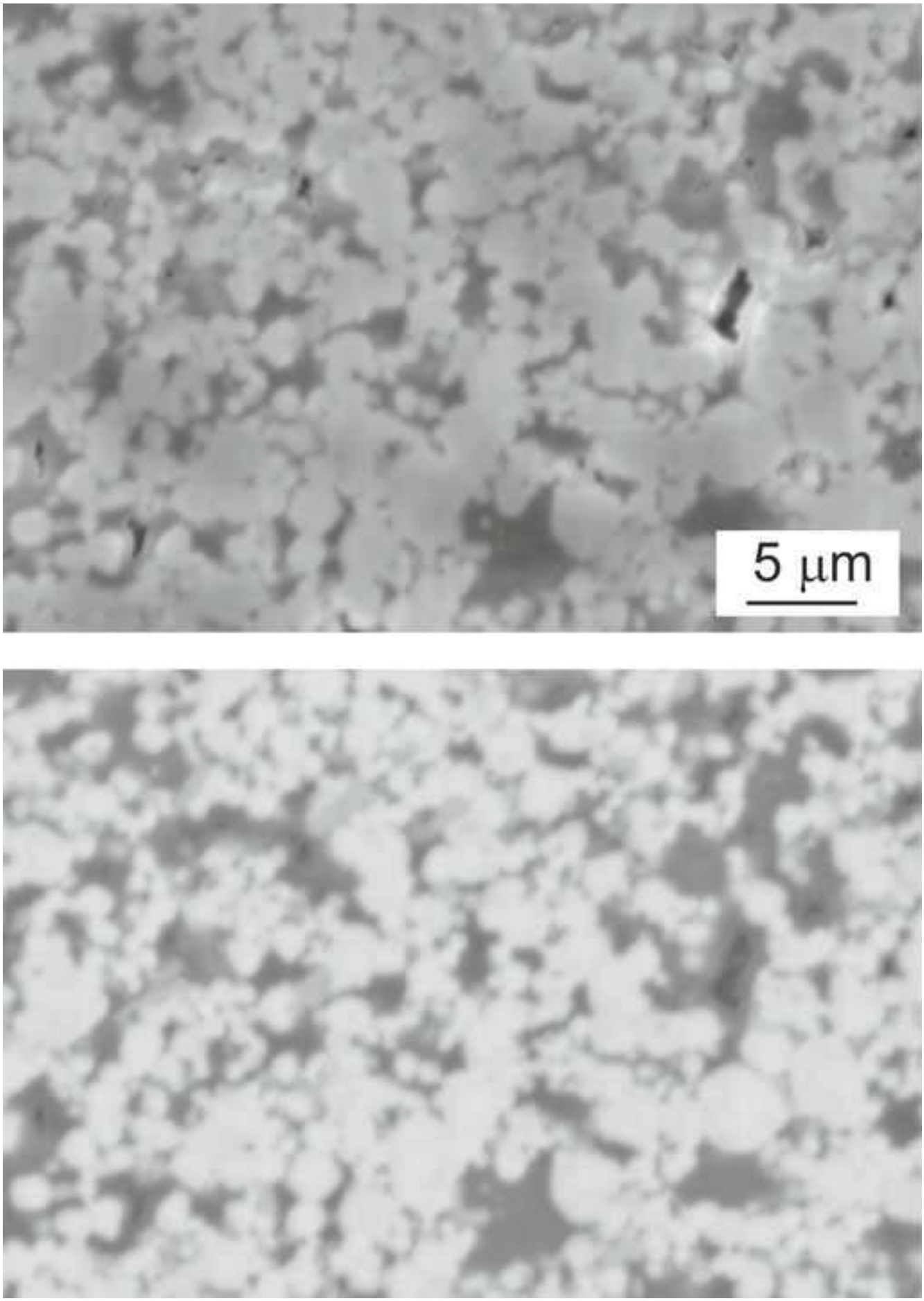

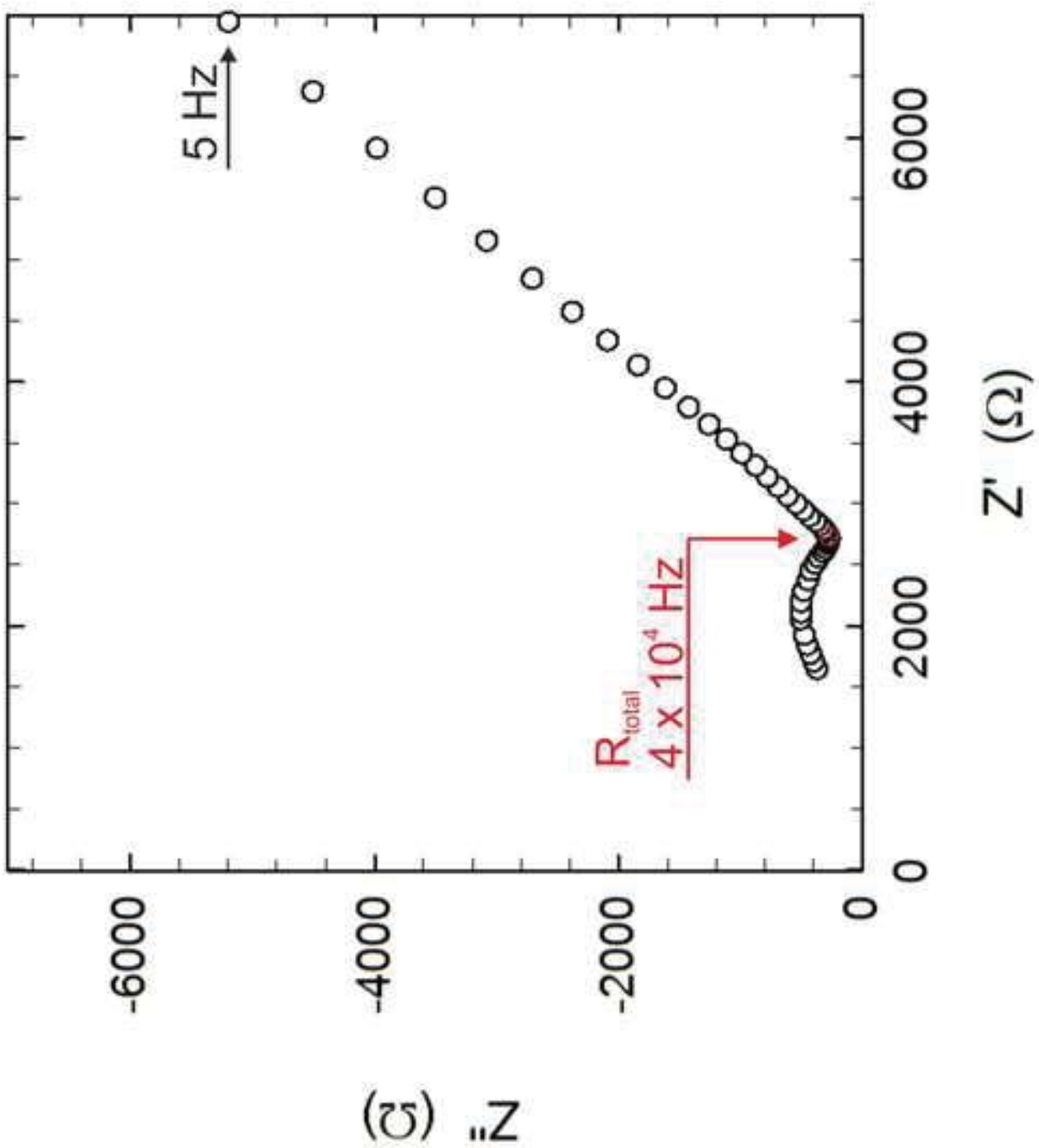

Figure 3

Figure 4

Click here to download Figure Figure 4.jpg

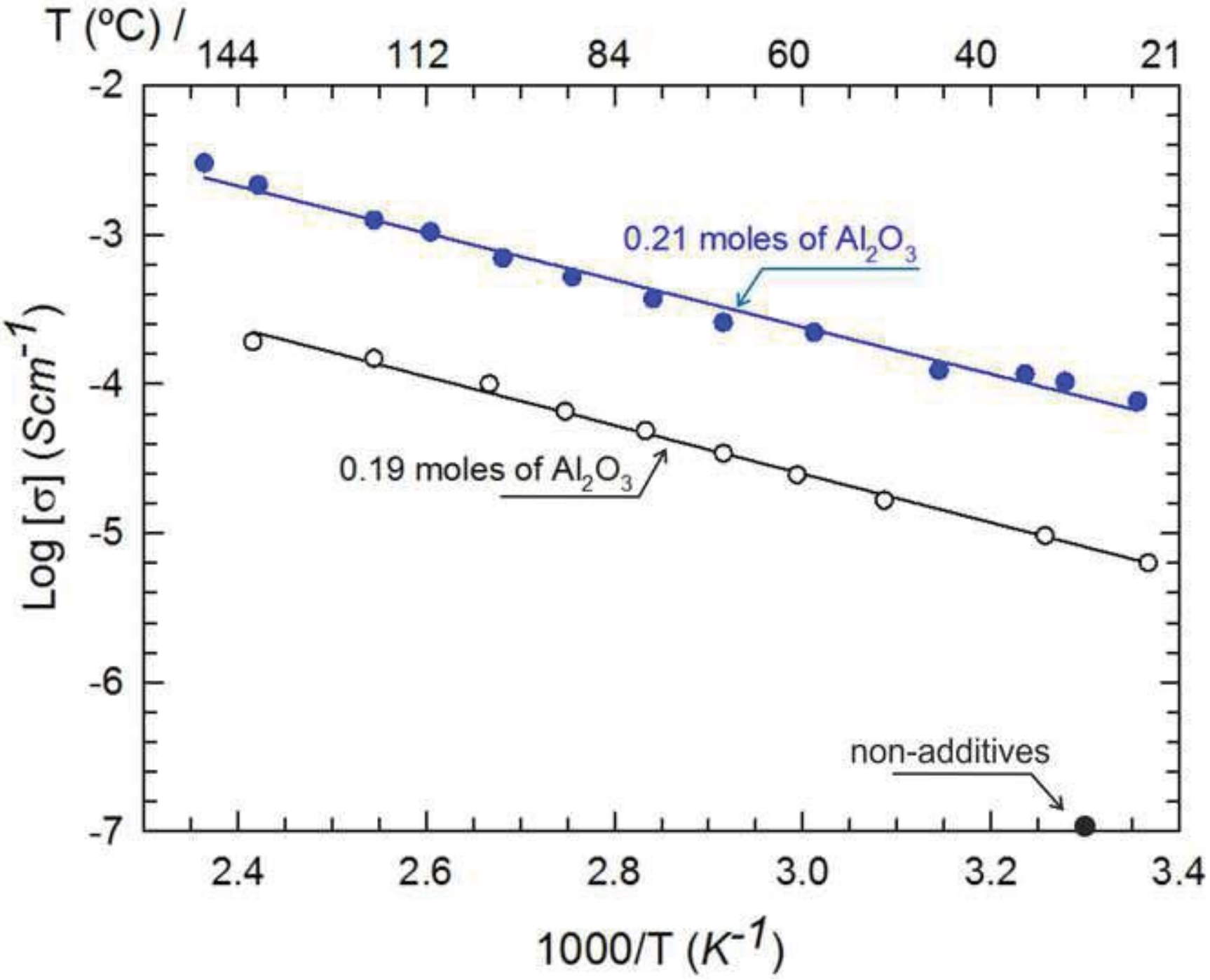

Table I. Relative density of LLCZT sintered at 900 °C with Li_3BO_3 and Al_2O_3.

Li_3BO_3 (mol)	Al_2O_3 (mol)	Relative density (g/cm^3)
-	-	56
0.80	-	58
	0.11	82
	0.19	94
	0.21	95
	0.22	83
0.75	0.21	87
0.70	0.21	85